



Yan, C., Sagisaka, M., Rogers, S. E., Hazell, G. D. A., Peach, J. A., & Eastoe, J. (2016). Shape Modification of Water-in-CO<sub>2</sub> Microemulsion Droplets through Mixing of Hydrocarbon and Fluorocarbon Amphiphiles. *Langmuir*, 32(6), 1421-1428. <https://doi.org/10.1021/acs.langmuir.5b03630>

Peer reviewed version

Link to published version (if available):  
[10.1021/acs.langmuir.5b03630](https://doi.org/10.1021/acs.langmuir.5b03630)

[Link to publication record in Explore Bristol Research](#)  
PDF-document

This is the author accepted manuscript (AAM). The final published version (version of record) is available online via ACS at <http://pubs.acs.org/doi/abs/10.1021/acs.langmuir.5b03630>

## University of Bristol - Explore Bristol Research

### General rights

This document is made available in accordance with publisher policies. Please cite only the published version using the reference above. Full terms of use are available:  
<http://www.bristol.ac.uk/pure/about/ebr-terms>

# Shape modification of water-in-CO<sub>2</sub> microemulsion droplets through mixing of hydrocarbon and fluorocarbon amphiphiles

Ci Yan<sup>◇</sup>, Masanobu Sagisaka<sup>†</sup>, Sarah Rogers<sup>§</sup>, Gavin Hazell<sup>◇</sup>, Jocelyn Peach<sup>◇</sup> and Julian Eastoe<sup>◇\*</sup>

<sup>◇</sup>School of Chemistry, University of Bristol, Bristol BS8 1TS, United Kingdom

<sup>†</sup>Department of Frontier Materials Chemistry, Graduate School of Science and Technology, Hirosaki University, Bunkyo-cho 3, Hirosaki, Aomori 036-8561, Japan

<sup>§</sup>Rutherford Appleton Laboratory, ISIS Facility, Chilton, Oxfordshire OX11 0QX, United Kingdom

## Abstract

An oxygen-rich hydrocarbon (HC) amphiphile has been developed as an additive for supercritical CO<sub>2</sub> (scCO<sub>2</sub>). The effects of this custom-designed amphiphile have been studied in water-in-CO<sub>2</sub> (w/c) microemulsions stabilised by analogous fluorocarbon (FC) surfactants, nFG(EO)<sub>2</sub>, which are known to form spherical w/c microemulsion droplets. By applying contrast-variation small-angle neutron scattering (CV-SANS), evidence has been obtained for anisotropic structures in the mixed systems. The shape transition is attributed to the hydrocarbon additive, which modifies the curvature of the mixed surfactant films. This can be considered as a potential method to enhance physico-chemical properties of scCO<sub>2</sub> through elongation of w/c microemulsion droplets. More importantly, by studying self-assembly in these mixed systems, fundamental understanding can be developed on the packing of HC and FC amphiphiles at water/CO<sub>2</sub> interfaces. This provides guidelines for the design of fluorine-free CO<sub>2</sub> active surfactants, and therefore, practical industrial scale applications of scCO<sub>2</sub> could be achieved.

## Introduction

Studies of self-assembly in supercritical carbon dioxide (scCO<sub>2</sub>) have been carried out over two decades since pioneering work in 1990s [1, 2, 3], and this field still attracts increasing interest as a promising solvent for nano-science [4, 5], drug delivery [6], and oil industries [7, 8].

Despite the fact that significant progress has been achieved in the development of CO<sub>2</sub>-philic surfactants [1-3, 9] and polymers [10, 11, 12], most of these species contain fluorocarbon (FC) surfactants or polymers, which is recognised as an important chemical group needed for CO<sub>2</sub>-philicity. As revealed by molecular dynamics simulations, this is possibly owing to favourable interactions between the quadrupoles of CF<sub>2</sub> segments and CO<sub>2</sub> molecules [13, 14], and also the bulkiness at the fluorocarbon (FC) structures which effectively prohibit interfacial penetration (intermixing) of water and CO<sub>2</sub> molecules [15, 16]. However, such a fluorine-rich molecular design has significant disadvantages for industrial scale applications due to economic and environmental concerns [17, 18, 19, 20]. On the other hand, despite only a few successful examples of stable dispersions with hydrocarbon (HC) surfactants in scCO<sub>2</sub> [20, 21, 22], development of efficient CO<sub>2</sub>-philic surfactants with minimum fluorine content still presents a great challenge, requiring a deeper insight to understand the general behaviour of surfactants in water/CO<sub>2</sub> systems.

Among a variety of approaches to obtain stable w/c microemulsions with reduced fluorine content surfactants [20-22, 23, 24, 25, 26], hybrid di-chain surfactants containing both hydrocarbon (HC) and fluorocarbon (FC) moieties have been identified as promising structures [23-26]. Moreover, hybrid surfactants have also been demonstrated to form rod-like micelles and increase viscosity of the scCO<sub>2</sub> medium [24, 26], which has potential for applications such as enhanced oil recovery (EOR) [7].

Recently, Sagisaka et al. [26] have reported a systematic study on the connections between

physiochemical properties of hybrid surfactants in scCO<sub>2</sub> and the balance of HC and FC moieties. By varying surfactant structure, the w/c microemulsion droplets show an interesting transition from spherical to rod-like shapes, which is controlled by the chain length of HC moieties. However, fundamental questions are still left unanswered: how does the balance of HC-FC moieties affect surfactant interfacial packing, which in turn enhances the elongation of microemulsion droplets; and how do these systems compare to previously reported perfluorinated surfactants [1-3, 9-12]?

It should be noted that, HC and FC alkanes de-mix due to unfavourable interactions [27,28]. Therefore, simply mixing HC and FC surfactants tends to destabilise microemulsions in scCO<sub>2</sub> [29].

In a recent study [30], contrast variation small-angle neutron scattering (CV-SANS) has been applied to investigate the behaviour of hydrotropes (primitive very hydrophilic hydrocarbon amphiphiles) in w/c microemulsions stabilised by FC surfactants. Analysis of the scattering profiles suggested interesting multiple-shell structures for the microemulsion droplets, with the hydrotropes forming an extra HC-rich layer between the water cores and FC film coronas at the interface. It is plausible to suggest that HC-FC hybrid surfactants tend to pack in a similar way, with the FC chains stretched towards the CO<sub>2</sub> bulk phase, and the HC moieties mainly acting as spacer groups at the interface. The presence of these interfacial spacer groups notably modifies the surfactant film curvature, resulting in formation of anisotropic self-assembly structures.

On the other hand, as noted in the literature [30], it is possible to obtain stable FC surfactant/hydrotrope mixtures in w/c microemulsions, by having hydrotrope molecules interact with the HC surfactant moieties. Therefore, if a suitable amphiphile is added at similar concentration to the surfactant, such an extra 'spacer' between the HC moieties should also

modify the curvature of surfactant films in a similar manner to the HC-FC hybrid surfactants; this could lead to anisotropic micelles.

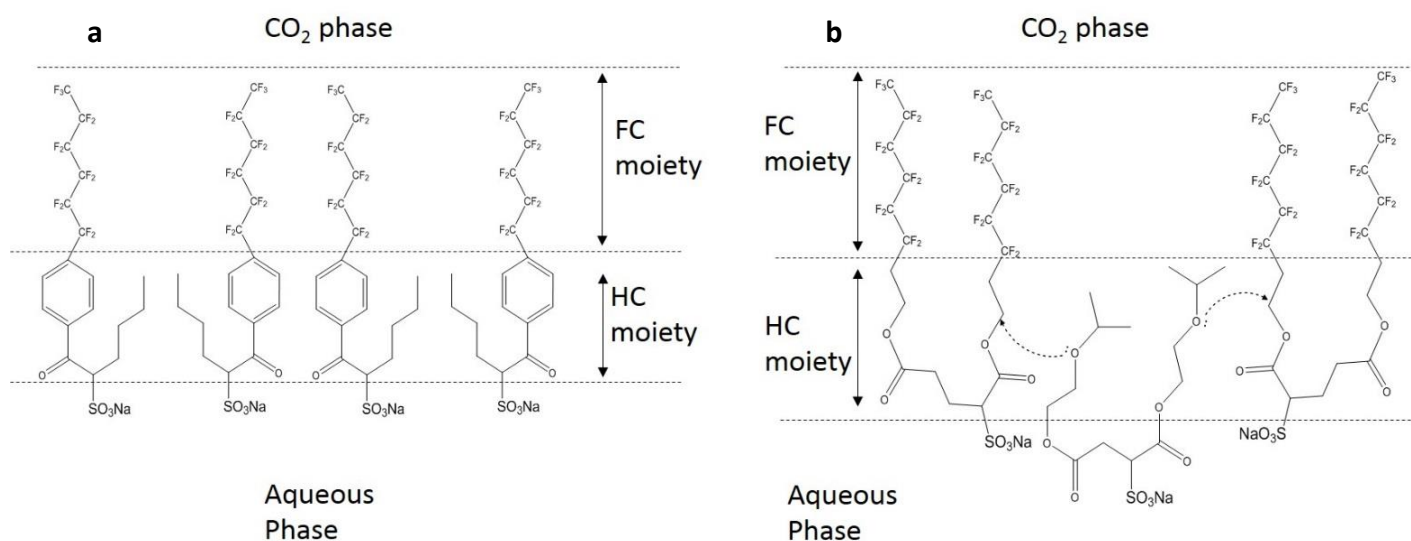


**Figure 1** schematics of surfactant packing at water/ $\text{CO}_2$  interfaces for different systems: **Figure a (left)** FC6-HC4 hybrid surfactants described in ref. 26, and **b (right)** 6FG(EO)<sub>2</sub> surfactants with di-IGSS, the co-adsorbing HC additive used in this paper.

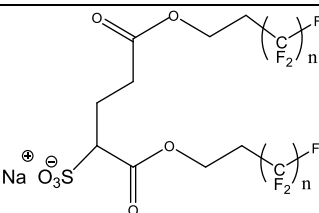
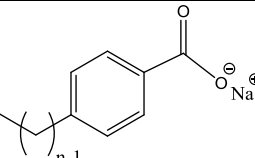
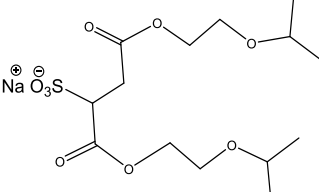
In this paper, SANS is applied to study the structures of microemulsion droplets in  $\text{scCO}_2$  with addition of two different HC amphiphiles: a new custom made amphiphile, di-IGSS, and  $\text{C}_8\text{Benz}$ , as used in ref. 30. The tail groups of di-IGSS are specifically designed to interact with the ethylene oxide (EO) groups of  $n\text{FG}(\text{EO})_2$  (Figure 1b), which should promote mixing of these HC moieties in the interfacial films. In contrast with the  $\text{C}_8\text{Benz}$  hydrotrope added systems, these favourable interactions are not to be expected between the alkyl groups in  $\text{C}_8\text{Benz}$  and the ethylene oxide groups in the surfactants.

The w/c microemulsions were formulated with a well-studied perfluorinated AOT analogue,  $n\text{FG}(\text{EO})_2$ , which is known to stabilise w/c microemulsions only as spherical droplets [9]. Hence, by investigating the effect of these different HC additives on the shape of w/c microemulsion droplets, deviations from the underlying spherical morphology can be explored, and the hypothesis about the packing of HC-FC amphiphiles as illustrated in Figure 1 can be tested.

## Experimental

### Materials

The structures of surfactants and co-adsorbed species in this study can be found in Table 1. Synthesis of hydrotropes and the FC surfactants can be found in literature [9, 40]. The di-IGSS is a custom made amphiphile, the method of synthesis and purification can be found in Supporting Information.

Compounds	Structure
nFG(EO) <sub>2</sub>	
Hydrotrope BenzC <sub>n</sub>	
di-IGSS	

**Table 1 Structures of surfactants and co-adsorbing species used by this study.**

### Preparation of w/c microemulsions

The surfactants were used at constant molarity in a pressure cell ( $M_{\text{surf}} = 0.017 \text{ mol L}^{-1}$  volume 20 mL), described below. The HC additives were mixed at constant molar ratio with respect to the surfactant ( $M_{\text{surf}} : M_{\text{additive}} = 2:1$ , or  $1:1$ ). In practice, the hydrotrope C<sub>8</sub>Benz was directly added to the cell, followed by addition of appropriate amounts of water which give rise to water: surfactant molar ratios W15 and W30. On the other hand, di-IGSS was introduced to the system in a solution of D<sub>2</sub>O (or mixed D<sub>2</sub>O/H<sub>2</sub>O for CV-SANS), followed by further injection of water (D<sub>2</sub>O or D<sub>2</sub>O/H<sub>2</sub>O mixture) to make up the water: surfactant ratio (W) of interest.

For experiments with variations in pressure, the CO<sub>2</sub> density was calculated using the Span-Wagner equation of state. For the experiments here CO<sub>2</sub> density varies within the range  $d_{\text{CO}_2} = 0.91\text{--}0.76 \text{ g cm}^{-3}$  at a constant temperature  $T=45^\circ\text{C}$  [31].

Transparent single phases were obtained for all di-IGSS added w/c microemulsions at  $T=45^\circ\text{C}$  and at pressures above  $P=150 \text{ bar}$ . However, the amphiphile di-IGSS itself does not show any solubility, or emulsifying power in the bulk CO<sub>2</sub> in the absence of the fluorinated surfactant, which suggests that di-IGSS can act as a co-surfactant or interfacial hydrotrope, and the partitioning into bulk scCO<sub>2</sub> is negligible.

On the other hand, with the C<sub>8</sub>Benz additive, the system appears initially to give translucent phases under stirring, but becomes clear on stopping the stirrer, indicating a Winsor I system with excess denser water separating and coexisting with the microemulsion.

#### *Pressure cell*

All samples were studied in a stainless steel cell with variable volume (12–20 mL) and path length 10 mm, controlled by a piston with an external hydraulic pump. Once filled with CO<sub>2</sub>, the pressure was measured by a built-in pressure transducer with accuracy  $\pm 1 \text{ bar}$ . Two sapphire windows fitted in parallel allow for visual observations of phase behavior and transmission of neutrons. Temperature was controlled at  $45^\circ\text{C}$  by a water bath flowing around a heating circuit in the cell body.

In order to obtain w/c microemulsions, the appropriate amount of pre-weighed surfactant and hydrotrope solution in D<sub>2</sub>O/H<sub>2</sub>O was fed into the cell to establish the  $W (= [\text{water}]/ [\text{surf}])$  of interest. Subsequently, the cell was sealed and liquid CO<sub>2</sub> was introduced, by pumping, at relatively low temperature  $\sim 5^\circ\text{C}$ , then re-equilibrated at  $45^\circ\text{C}$  under magnetic stirring. The inlet line was closed once the pressure reached 120 bar, and under these conditions CO<sub>2</sub> is in

a supercritical state. The pressure could be further increased using a hydraulic pump, up to a maximum of 450 ( $\pm 5$ ) bar, which allowed stable w/c microemulsions to be formulated.

## SANS

Small-Angle Neutron Scattering (SANS) is a powerful technique to study the assembly, alignment, dispersion and mixing of nanoscale condensed matter typically over length scales 1-50 nm. In this paper, SANS has been applied as the primary characterization method, due to following advantages:

1. High-penetrating power of neutrons, ideal to facilitate the use of complex sample-environment equipment, which allows extremes of pressure to be created and sustained for the experiments with  $\text{scCO}_2$ .
2. The scattering of neutrons is related to interactions with nuclei in the sample, which allows isotopes of the same element to be distinguished with a significant difference in the scattering lengths of neutrons for  $^1\text{H}$  compared to  $^2\text{H}$ . Therefore, the structure of water-containing microemulsion droplets can be confirmed by scattering with different domains being highlighted by isotopic labelling [32].

For SANS experiments, the scattering intensity  $I(Q)$  is plotted as a function of the momentum of transfer,  $Q$ , which can be described by [33]:

$$Q = \frac{4\pi}{\lambda} \sin \frac{\theta}{2} \quad (1)$$

where  $\theta$  is the scattering angle and  $\lambda$  the incident neutron wavelength, and

$$I(Q) \propto P(Q)S(Q) + B_{inc} \quad (2)$$

$B_{inc}$  is the background incoherent scattering,  $S(Q)$  is the structure factor related to inter-particle interactions. In this study, the systems were at low concentration in a non-polar medium, therefore,  $S(Q)$  can be neglected ( $S(Q) \sim 1$ ). [32, 33].  $P(Q)$  is the form factor which



describes the internal structure of scattering particles. Form factors are closely related to the contrast of scattering, which arises from the difference in scattering length density (SLD, or  $\rho$ ) between adjacent phases:

$$\rho = \sum_i b_i/V_m \quad (3)$$

$b_i$  are the nuclear scattering lengths, which depend on the identity of the nuclei of different isotopes as given in the literature [34], and  $V_m$  is the molecular volume, which can be determined from the mass density of each component. Therefore, as mentioned earlier in this section, the scattering contrast can be varied to highlight the region of interest, via an exchange of isotopes ( $^1\text{H}$  and  $^2\text{H}$ ) for different components in the system.

SANS measurements were performed using instruments LOQ [35] and SANS2D [36] at the ISIS spallation source, Rutherford Laboratory, UK. SANS2D spans a  $Q$  range of  $0.002 < Q < 1 \text{ \AA}^{-1}$  with neutron wavelength  $\lambda$  of  $2.2\text{-}16 \text{ \AA}$ , whereas for LOQ,  $0.008 < Q < 0.25 \text{ \AA}^{-1}$  and  $\lambda$  is within the range  $2\text{-}14 \text{ \AA}$ . The path length was 10 mm, and sample to detector distance was 4.1 m. Transmissions were in the range 0.9-0.7 over the wavelengths employed (see Figure S7 in Supporting Information). All scattering data were normalized for the sample transmission, empty cell and  $\text{CO}_2$  background and put on an absolute intensity  $I(Q)/\text{cm}^{-1}$  scale using standard procedures [37]. Once w/c microemulsions were obtained at the appropriate conditions, the systems were equilibrated with stirring for 5 min before SANS measurements were made.

Results were fitted by the program SASview using built-in form factor models (found in Supporting Information), the datasets were analysed over an appropriate  $Q$ -range so that most data points should have a standard error  $< 10\%$  ( $20\%$  for samples in core-shell contrasts, due to the limited instrumental resolution against relatively poor contrast) for the clarity of presentation and accuracy of analysis. The SLDs of each component were calculated from the

density and chemical composition, and were constrained for fitting ( $\rho_{\text{co-adsorb}} = 1.3 \times 10^{-6} \text{ \AA}^{-2}$ ,  $\rho_{\text{surf}} = 3.5 \times 10^{-6} \text{ \AA}^{-2}$ , and  $\rho_{\text{D}_2\text{O}} = 6.3 \times 10^{-6} \text{ \AA}^{-2}$ . The bulk SLD  $\rho_{\text{CO}_2} = 2 \times 10^{-6} \text{ \AA}^{-2}$  when  $\text{CO}_2$  density  $d_{\text{CO}_2} = 0.76 \text{ g cm}^{-3}$ , and  $2.3 \times 10^{-6} \text{ \AA}^{-2}$  when  $d_{\text{CO}_2} = 0.92 \text{ g cm}^{-3}$ ). It should be noted that the SLD of microemulsion droplets was set as  $\rho_{\text{drop}} = 3.9 \times 10^{-6} \text{ \AA}^{-2}$ , by considering the contribution from the  $\text{D}_2\text{O}$  core, the co-adsorbing HC species and the surfactant layer.

## Results and discussion

### *Water-in- $\text{CO}_2$ microemulsions with di-IGSS additive*

The SANS data and fitting for the di-IGSS added w/c microemulsions ( $M_{\text{surf}} : M_{\text{IG}} = 2:1$ ) at W30 are presented in Figure 2. Results obtained from a  $\text{D}_2\text{O}$  core contrast clearly show gradients close to  $D = -\frac{d \log I(Q)}{d \log Q} = -1$  over the low Q regime, which should correspond to elongated structures [33]. Whereas for spherical particles, a  $D = -4$  dependence should be obtained, and for systems with comparable sizes and no inter-droplet interaction, the gradient should quickly decay to  $D = 0$  at low Q regime ( $Q \sim 0.02 \text{ \AA}^{-1}$ ) [9].

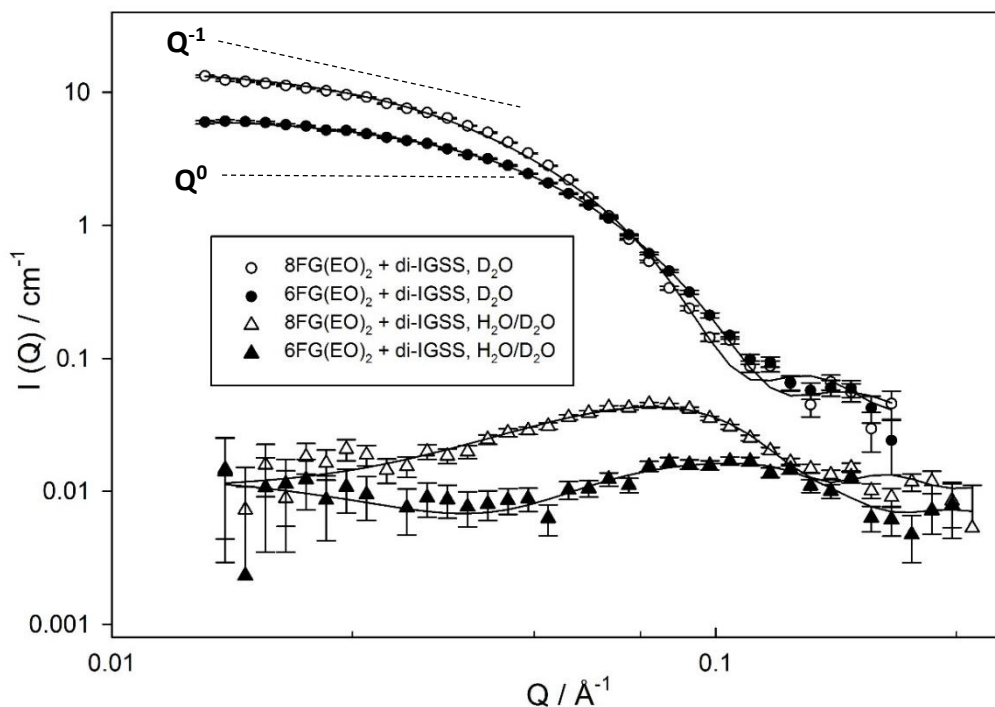


**Figure 2 SANS data for the w/c microemulsions with D<sub>2</sub>O and H<sub>2</sub>O/D<sub>2</sub>O mixed (8:2 mass ratio) core at W30 stabilised by 8FG(EO)<sub>2</sub> and 6FG(EO)<sub>2</sub> (both datasets multiplied by 8×) with di-IGSS additives (2:1 molar ratio), the data were fitted using ellipsoidal (D<sub>2</sub>O core) and core-shell ellipsoidal (mixed core) form factor models. Experiments were performed at 350 bar, 45 °C.**

The systems have also been examined at core-shell contrast with H<sub>2</sub>O/D<sub>2</sub>O mixed core, as compared in Table 2, contrast variation SANS shows good self-consistency. More importantly, the distinguishable peaks with core-shell contrasts are clear indications of relatively monodispersed systems (with a Schulz distribution  $\sigma/R_{av} < 0.20$ ), which rules out the possibility of highly polydisperse spherical structures.

The SANS data were analysed using ellipsoid and core shell ellipsoid form factor models, and the results are summarised in Table 2. It should be noted that, by applying the form factor model for rod structures, the analyses give similar cross section radii and aspect ratio as for to ellipsoid form factors. This is possibly owing to the relatively low aspect ratio, i.e. the ellipsoids cannot be easily distinguished from rod-like structures. Nevertheless, the anisotropic microemulsion droplets were considered to be ellipsoids, based on the assumption that the

elongation is attributed to the modification on the surfactant films, which should result in a gradual deformation from sphere to ellipsoid, instead of extreme rod shapes.

In Table 2, the fit parameters have also been compared with results from Guinier analyses (plots in Supporting Information), from which the cross section radius ( $R$ ) and length ( $L = 2 \times$  the radius in polar axis for an ellipsoidal particle, i.e.,  $L \sim 2R_a$ ) of aggregates with elongated structures can be obtained from the radius of gyration ( $R_g$ ) as shown below [38]:

For the low  $Q$  regime, Guinier approximation can be expressed as:

$$\ln[I(Q)] \propto -\frac{Q^2 R_g^2}{3}, \text{ where } R_g^2 = \frac{L^2}{12} + \frac{R^2}{2} \quad (4)$$

And for the intermediate- $Q$ :

$$\ln[I(Q) \cdot Q] \propto -\frac{Q^2 R_{chara}^2}{2}, \text{ where } R_{chara}^2 = \frac{R^2}{2} \quad (5)$$

$R_{chara}$  is the characteristic dimension of the particle, which is related to the cross sectional radius ( $R$ ) of elongated microemulsion droplets.

Systems	6FG(EO) <sub>2</sub> + di-IGSS	8FG(EO) <sub>2</sub> + di-IGSS
R (Guinier) / Å	31	35
L (Guinier) / Å	96	176
Fitted R <sub>a</sub> (±1) / Å (D <sub>2</sub> O core)	67	95
Fitted R <sub>b</sub> (±1) / Å (D <sub>2</sub> O core)	32	35
R <sub>a</sub> : R <sub>b</sub> (D <sub>2</sub> O core)	2.1	2.7
Fitted R <sub>a</sub> (±1) / Å (H <sub>2</sub> O/D <sub>2</sub> O core)	57	93
Fitted R <sub>b</sub> (±1) / Å (H <sub>2</sub> O/D <sub>2</sub> O core)	23	27
Shell thickness (±1) / Å (H <sub>2</sub> O/D <sub>2</sub> O core)	9	11
$\Sigma \times 10^6 / (\text{Å}^{-1})$	1060	995
SA / Å <sup>2</sup>	106	100
N <sub>agg</sub>	276	501

**Table 2 Results of Guinier analyses compared with model fit parameters based on ellipsoidal and core-shell ellipsoidal form factor models for w/c microemulsions stabilised by the nFG(EO)<sub>2</sub> surfactant at W30 (Figure 2). The surface area per surfactant (SA) and aggregation number (N<sub>agg</sub>) are also estimated based on Porod analyses (Figure 3).**

In general, a good agreement is observed between the fit parameters from the ellipsoidal form factor model and Guinier analysis. Based on both analysis methods the 8FG(EO)<sub>2</sub> stabilised system appears to give a relatively more extended elongation with a higher aspect ratio of radii in polar and equatorial axis (R<sub>a</sub>: R<sub>b</sub>), as compared to the short chain surfactant analogue. The interfacial properties of surfactants in w/c microemulsions with the di-IGSS additive have been further investigated by analysing the data over the high-Q Porod regime, from which, the interfacial coverage of surfactant molecules (SA), and aggregation number (N<sub>agg</sub>) can be estimated and compared to literature values for related surfactants [9].

The Porod analysis is based on assumption of a sharp microemulsion droplet interface, and

the approximation that the scattering intensity ( $I(Q)$ ) at high  $Q$  regime is sensitive to the total interfacial area ( $S_{tot}$ ) in the system, as obtained in Equation 6 [39].

$$\{I(Q)Q^4\}_{Q \rightarrow \infty} = 2\pi(\Delta\rho)^2\Sigma \quad (6)$$

where  $\Sigma$  is the total area per unit volume ( $\Sigma = S_{tot}/V_{tot}$ ,  $S_{tot}$  is the total interfacial area, and  $V_{tot}$  is the system volume), and  $\Delta\rho$  is the difference of SLD at the interface, which can be obtained as  $\Delta\rho = \rho_{drop} - \rho_{bulk}$ .

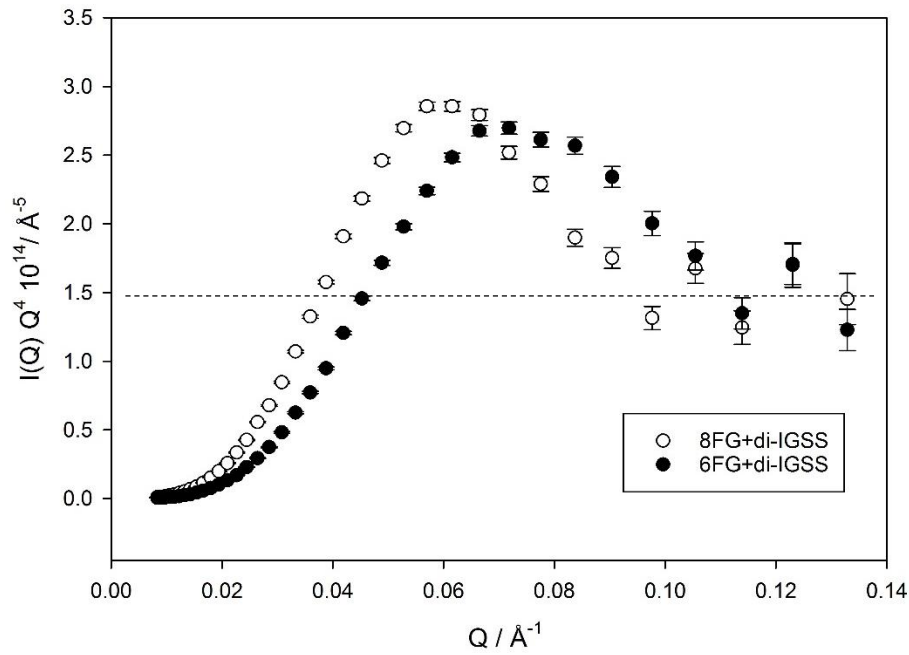


**Figure 3** Porod plot for microemulsions stabilised by 8FG(EO)<sub>2</sub> and 6FG(EO)<sub>2</sub> at W30 (D<sub>2</sub>O core) with the di-IGSS additive (2:1 molar ratio) as obtained in Figure 2. The dashed line shows an estimation of  $I(Q)Q^4$  at high  $Q$ .

Having obtained  $\Sigma$  from the total interfacial area  $S_{tot}$ , and the number of adsorbed species per unit volume  $N_s$ , the surface area per surfactant molecule ( $SA$ ) can be estimated as:

$$SA = \frac{\Sigma}{N_s} \quad (7)$$

It should be noted that, this approach only considers the surfactants as adsorbed species at the interface, since the bulky fluorocarbon chains should dominate the surface coverage contributing to the scattering. Thus, the number of interfacially adsorbed species can be

estimated from the concentration of surfactant ( $M_{\text{surf}} = 17\text{mM}$ ). However, if contributions from the hydrocarbon additives are also considered the average molecular surface area  $SA$  would be lower than the values predicted in Table 3.

Furthermore, as the surface area per microemulsion droplet ( $A$ ) can be calculated from the core radius ( $R_a$  and  $R_b$ ) obtained from fitting, the aggregation number of surfactants,  $N_{\text{agg}}$ , can also be estimated based on  $A$  and  $SA$ :

$$N_{\text{agg}} = \frac{A}{SA} = 4\pi \left( \frac{(R_a R_b)^{1.6} + (R_a R_b)^{1.6} + (R_b R_b)^{1.6}}{3} \right)^{1/1.6} \cdot \frac{1}{SA} \quad (8)$$

As obtained in Table 2, analysis from the Porod plots have shown an average interfacial area  $SA \sim 100 \text{ \AA}^2$  per surfactant, which is significantly reduced compared to simple w/c microemulsions with the same surfactant on its own ( $SA \sim 123 \text{ \AA}^2$ ) [9]. Such a reduction in  $SA$  and increase in  $N_{\text{agg}}$  is consistent with a reduction of surfactant film curvature and increased anisotropy of the microemulsion droplets.

#### *Optimisation of di-IGSS induced elongation*

The effects of di-IGSS were further studied with a variation of the conditions applied, which could potentially enhance the elongation.

At first, the 8FG(EO)<sub>2</sub> stabilised systems were studied with increasing levels of di-IGSS ( $M_{\text{surf}} : M_{\text{di-IGSS}} \sim 1:1$ ), and the water contents were varied from  $W15 \sim W45$ .

As revealed by studies with water-in-oil (w/o) microemulsions [40, 41], elongation of microemulsion droplets can be enhanced with a higher concentration of hydrotropic additives at lower water contents. Therefore, by increasing the amount of di-IGSS, a more significant effect was expected on the w/c microemulsion structure. However, the SANS results (Figure 4) have shown quite the opposite: despite the fact that results can still be fitted using an ellipsoidal form factor model, the microemulsion droplets at  $W30$  ( $M_{\text{surf}} : M_{\text{di-IGSS}} = 1:1$ )

appeared to be less elongated as compared to the 8FG(EO)<sub>2</sub> stabilized system with the same  $W$  ratio but lower di-IGSS content as obtained in earlier section ( $M_{\text{surf}} : M_{\text{di-IGSS}} = 2:1$ , as shown in Figure 2). On the other hand, the effect of  $W$  ratio also appeared to be difficult to determine in these w/c systems: although the aspect ratios were found to notably increase with reduced  $W$  ( $R_a : R_b$  up to 3.0 as the water content decreased from  $W45$  to  $W22$ ), however, on reducing the water content further to  $W15$ , the elongation was not enhanced.

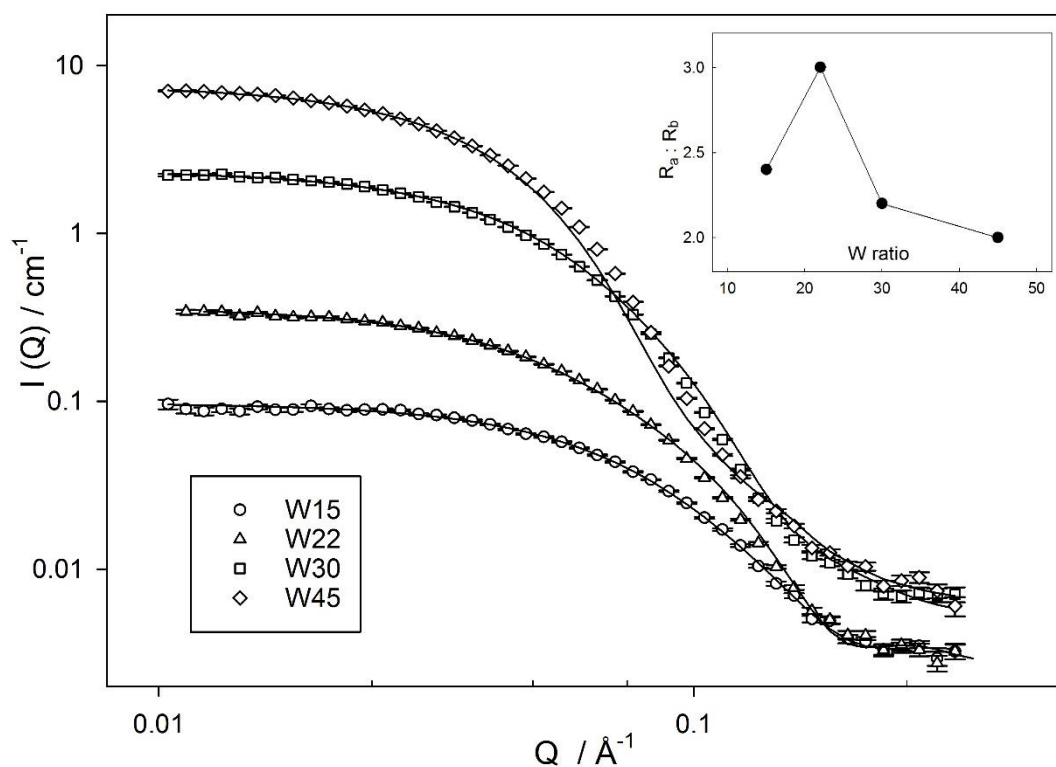


**Figure 4** SANS data obtained w/c microemulsions stabilised by 8FG(EO)<sub>2</sub> with added di-IGSS, at 350 bar, 45°C. The water: surfactant molar ratio was varied from  $W15$  to  $W45$  (the datasets for  $W30$  and  $45$  have been multiplied by  $3\times$  for the clarity of presentation), the aspect ratios between the polar and equatorial radius have also been plotted as a function of  $W$  in the inset, fit parameters for the data can be found in Supporting Information.

The results seem to suggest that the droplet anisotropy of w/c microemulsions may not be correlated with the content of the amphiphilic additives,  $M_{\text{di-IGSS}}$ . This is in contrast to analogous w/o systems where a general trend is observed with increasing hydrotrope content



[40]. This is likely to arise from the partial mixing between the additive and the EO moieties of  $n\text{FG}(\text{EO})_2$ , and in this case, the geometry of surfactant layer can be influenced by an array of factors such as surfactant chain length, interfacial composition, and core size, etc.

In comparison, the effect of hydrotropes in w/o systems, which are expected to penetrate through the HC surfactant film and modify the curvature directly, appeared to be more predictable [40, 41].

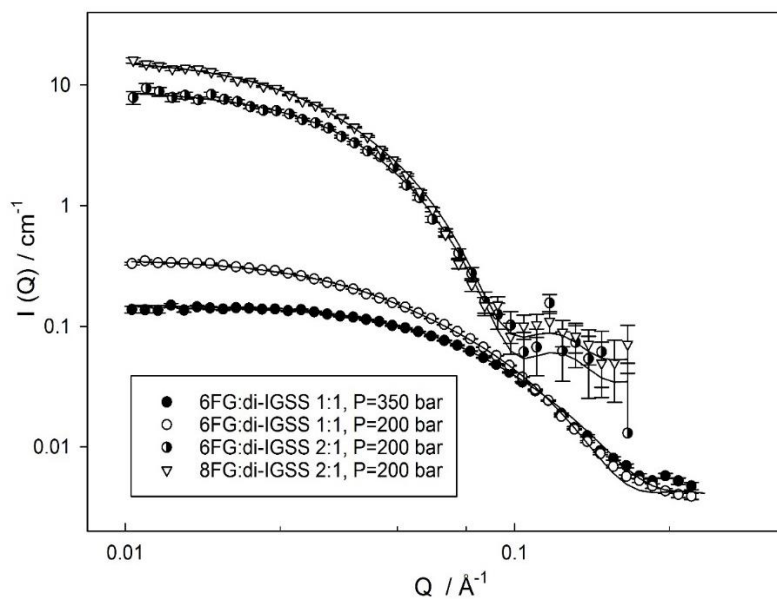


**Figure 5 SANS results obtained for w/c microemulsions at W30 stabilised by 6FG(EO)<sub>2</sub> and 8FG(EO)<sub>2</sub> with added di-IGSS, the bulk density of CO<sub>2</sub> has been varied by pressure (at 45°C,  $d_{\text{CO}_2} = 0.76 \text{ g cm}^{-3}$  at 200 bar and  $d_{\text{CO}_2} \sim 0.91 \text{ g cm}^{-3}$  at 350 bar). Datasets correspond to samples at  $M_{\text{surf}}:M_{\text{IG}} \sim 2:1$  have been multiplied by 20× for the clarity of presentation.**

In a previous study [42], it was shown that variation of the CO<sub>2</sub> bulk density could result in effects on the surfactant films, and even the microemulsion droplet shapes. Here, the effect of bulk density has also been examined under a reduced pressure  $P = 200 \text{ bar}$  (corresponding to a bulk density  $d_{\text{CO}_2} \sim 0.76 \text{ g cm}^{-3}$  at 45°C). Interestingly, as compared below in Table 3, all systems obtained at reduced  $d_{\text{CO}_2}$  appeared to exhibit enhanced elongation, in particular, for the 6FG(EO)<sub>2</sub> stabilised system with  $M_{\text{surf}} : M_{\text{di-IGSS}} \sim 1:1$  and W30, as the pressure was reduced

from 350 to 200 bar, the aspect ratio of the structures increase from  $R_a: R_b = 2.9$  to 4.3.

In summary, although the effects of hydrotropic additives in w/c microemulsions did not appear to be as apparent as those in w/o based systems [40, 41], notably enhanced droplet elongation was obtained at lower pressures. This is consistent with previous studies on the effects of bulk densities on self-assembly in scCO<sub>2</sub> [42], and could be considered as optimized conditions for anisotropic structures in w/c microemulsions.

Surfactant	$R_a(\pm 1)/\text{\AA}$	$R_b(\pm 1)/\text{\AA}$	$R_a: R_b$	$M_{\text{surf}}: M_{\text{di-IGSS}}$	Pressure / bar
6FG(EO) <sub>2</sub>	64	32	2.0	2:1	200
6FG(EO) <sub>2</sub>	67	32	2.1	2:1	350
6FG(EO) <sub>2</sub>	82	19	4.3	1:1	200
6FG(EO) <sub>2</sub>	46	16	2.9	1:1	350
8FG(EO) <sub>2</sub>	123	44	2.8	2:1	200
8FG(EO) <sub>2</sub>	95	35	2.7	2:1	350

**Table 3** Fit parameters using the ellipsoidal form factor model for SANS data presented in Figure 2 in comparison to those obtained at 350 bar (SANS data were obtained from the w/c microemulsions at W30 stabilised by 6FG(EO)<sub>2</sub> and 8FG(EO)<sub>2</sub> with di-IGSS additive at molar ratio  $M_{\text{surf}}: M_{\text{di-IGSS}} = 1:1$  and 2:1.)

#### *Water-in-CO<sub>2</sub> microemulsions with C<sub>8</sub>Benz additive*

The effects of adding a hydrotrope, C<sub>8</sub>Benz have also been examined in w/c microemulsions stabilised 8FG(EO)<sub>2</sub> with molar ratio  $M_{\text{surf}}: M_{\text{hydro}} \sim 2:1$  and various *W* ratio (W15 and W30), to compare with the di-IGSS additive shown in Figure 2.

As shown in Figure 6, similar to the di-IGSS added systems, a gradient  $\frac{d \log I(Q)}{d \log Q} \sim -1$  is obtained in the low-Q Guinier region, which could correspond to anisotropic microemulsion droplets in both W15 and W30 systems. However, sharp increases of  $I(Q)$  were also obtained at  $Q \sim 0.01 \text{ \AA}^{-1}$ . This indicates existence of larger colloidal aggregates, and is consistent with an increase in light scattering from the sample (translucency). The scattering profiles have been analysed with the ellipsoidal form factor model, and the results are summarised in Table 4.

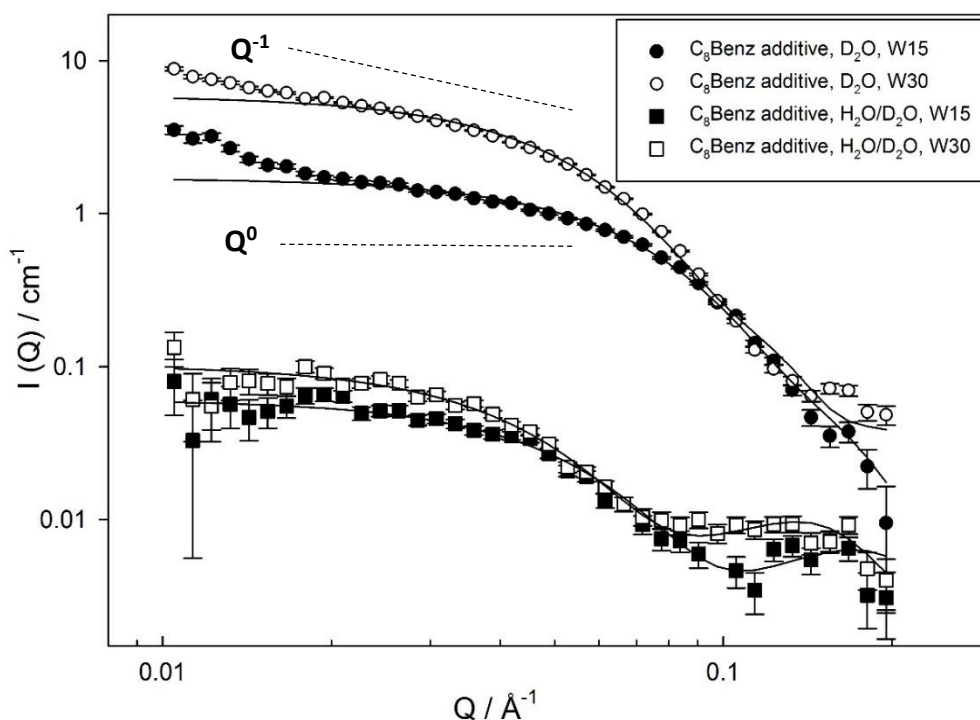


**Figure 6** SANS data for w/c microemulsions stabilised by 8FG(EO)<sub>2</sub> with added C<sub>8</sub>Benz at different W ratios, the systems have been examined with D<sub>2</sub>O (datasets multiplied by 8×) and H<sub>2</sub>O/D<sub>2</sub>O mixed cores, and the results are fitted by ellipsoidal and core-shell ellipsoidal form factor models. Experiments were performed at 350 bar, 45 °C.

W ratio	core	R <sub>a</sub> (±1) / Å	R <sub>b</sub> (±1) / Å	Shell thick (±1) / Å
15	H <sub>2</sub> O/D <sub>2</sub> O	44	14	11
15	D <sub>2</sub> O	54	21	-
30	H <sub>2</sub> O/D <sub>2</sub> O	60	17	11
30	D <sub>2</sub> O	75	29	-

**Table 4** Fitting parameters for the C<sub>8</sub>Benz containing microemulsions as shown in Figure 6. Analyses were based on the ellipsoidal form factor model.

Interestingly, although both the phase behaviour and SANS for the system at W15 seemed to suggest saturation has been reached for the dispersion of water within the microemulsion droplets. However, by comparing SANS for systems at W15 and W30, a clear shift of scattering profile is obtained for both contrasts with D<sub>2</sub>O and H<sub>2</sub>O/D<sub>2</sub>O cores, which suggests an expansion of core radius with increasing water content.

It should be noted that, for simple systems stabilised by the surfactant 8FG(EO)<sub>2</sub> alone, stable w/c microemulsions were obtained up to water content  $\sim W/80$  [9]. Apparently, the hydrotropes destabilised the microemulsions in this C<sub>8</sub>Benz containing system: despite effectively promoting anisotropic microemulsions, the accumulation of C<sub>8</sub>Benz could also give rises to disruption in the surfactant films preventing penetration of CO<sub>2</sub> and water molecules into the interface [15, 16].

On the other hand, by introducing additional H<sub>2</sub>O/D<sub>2</sub>O to the systems excess aqueous phases were still obtained, then the saturated hydrotropes in the aqueous cores would be effectively diluted owing to partitioning into phase separated water. This leads to an expansion of core radius.

## Conclusions

In this work, effects of two different co-adsorbing HC amphiphiles have been investigated in w/c microemulsions stabilised by fluorocarbon (FC) surfactants of the type nFG(EO)<sub>2</sub>. As revealed in a previous study [9], when used alone analogues of this kind are only capable of stabilising spherical w/c microemulsion droplets.

By applying CV-SANS, anisotropic micellar structures have been confirmed in all systems with the hydrocarbon (HC) additives, and by applying the custom-designed amphiphile, di-IGSS, notable enhancement was obtained in both elongation and stability of the microemulsions, as compared to systems with a non-interacting C<sub>8</sub>Benz hydrotrope.

Optimization of conditions to obtain anisotropic w/c micelles using the di-IGSS additive were also investigated. With reduced bulk CO<sub>2</sub> density, notable enhancement on the elongation of anisotropic structures were found in all systems. In particular, with a 6FG(EO)<sub>2</sub> stabilised system, ellipsoidal micellar structures were obtained with significant aspect ratios  $R_a : R_b$  up to ~4.3 as the pressure was reduced from 350 to 200 bar at 45 °C. However, variations in the concentration of the HC additives did not appear to give the same effects as seen in w/o systems with hydrotropes [40, 41]. This is possibly due to the partial mixing between the additives and FC surfactants at water/CO<sub>2</sub> interface, as proposed in the literature [30].

These observations appear to be consistent with the hypothesis about packing of HC and FC amphiphiles at water/scCO<sub>2</sub> interface as illustrated in Figure 1. This new custom designed amphiphile di-IGSS has been shown as effective modifier for the surfactant film curvature, resulting in formation of anisotropic structures in scCO<sub>2</sub>, this may be attributed to the following:

1. Good compatibility with the HC moieties of hybrid surfactants, which enhances the mixing through favorable interactions between the EO groups.

2. Modest molecular volume of the di-chain structure, which induces notable effects on the surfactant packing without disrupting the system stability.

3. The packing of di-IGSS at the interface may prohibit the penetration of water molecules.

It should be noted, that the EO groups in nFG(EO)<sub>2</sub> analogues are actually a common structure which can be found in a number of CO<sub>2</sub>-active surfactants, such as di-CF<sub>n</sub>, hybrid CF<sub>2</sub>-AOT4 [23, 25], and give rise to favourable interactions. Therefore, the effect of di-IGSS found in this study should not be limited to the nFG(EO)<sub>2</sub> analogues, but can also be expected with a range of perfluorinated, or HC-FC hybrid surfactants.

Moreover, in a number of studies based on water-in-oil (w/o) microemulsions, polymer additives containing EO functional groups have shown interesting behaviour in surfactant films [43] and spherical-ellipsoidal shape transitions of microemulsion droplets have also been reported [44, 45]. Such polymers may also be potential candidates as HC additives, and the effect of mixing with FC surfactants in w/c microemulsions should be tested in future experiments.

In this study, stable w/c microemulsions were obtained with interesting anisotropic structures through mixing of HC and FC amphiphiles. This is not only a promising approach to obtain micellar elongation in scCO<sub>2</sub>, which effectively enhances the viscosity of the medium [11, 24]. More importantly, strong evidence has been found for a possible explanation for the self-assembly of HC and FC amphiphiles at the interface. This may be connected to behaviour of hybrid HC-FC surfactants, and potentially used to guide the design of efficient CO<sub>2</sub>-active surfactants with minimum fluorine content, and hence facilitate large scale practical applications of scCO<sub>2</sub>.

### Supporting Information.

Synthesis for di-IGSS, with characterization by  $^1\text{H-NMR}$  and aqueous phase surface tension. Additional SANS data for di-IGSS aqueous solutions and water-in- $\text{CO}_2$  microemulsions, details of SANS structural models. Additionally, example neutron transmission versus wavelength data are given for a water-in- $\text{CO}_2$  microemulsion. This material is available free of charge via the Internet at "<http://pubs.acs.org>."

### Author information

Corresponding Author. \*E-mail [Julian.eastoe@bristol.ac.uk](mailto:Julian.eastoe@bristol.ac.uk); FAX +44-117-928-9180

Notes. The authors declare no competing financial interest.

### Acknowledgement

This project was supported through EPSRC EP/I018301/1 under the G8 Research Councils Initiative for Multilateral Research Funding –G8-2012. The authors thank the UK Science and Technology Facilities Council (STFC) for allocation of beamtime at ISIS and grants toward consumables and travel. This work benefited from SasView software, originally developed by the DANSE project under NSF award DMR-0520547.

## References

---

- 1 Consan K.A., Smith R.D., Observations on the solubility of surfactants and related molecules in carbon dioxide at 50°C, *J. Supercrit. Fluids*, 1990; 3: 51-65
- 2 Hoefling T.A., Enick R.M., Beckman E.J., Microemulsions in near-critical and supercritical carbon dioxide, *J. Phys. Chem.*, 1991; 95: 7127-7129
- 3 Harrison K., Goveas J., Johnston K.P., O'Rear E.A., Water-in-Carbon Dioxide Microemulsions with a Fluorocarbon-Hydrocarbon Hybrid Surfactant, *Langmuir*, 1994; 10: 3536-3541
- 4 Lim K.T., Hwang H.S., Lee M.S., Lee G.D., Hong S., Johnston K.P., Formation of TiO<sub>2</sub> nanoparticles in water-in-CO<sub>2</sub> microemulsions, *Chem. Commun.*, 2002; 1528-1529
- 5 Zhang J., Han B., *J. Supercrit. Fluids*, Supercritical CO<sub>2</sub>-continuous microemulsions and compressed CO<sub>2</sub>-expanded reverse microemulsions, 2009; 47: 531-536
- 6 Chen A.Z., Tang N., Wang S.B., Kang Y.Q., Song H.F., Insulin-loaded poly-l-lactide porous microspheres prepared in supercritical CO<sub>2</sub> for pulmonary drug delivery, *J. Supercrit. Fluids*, 2015; 101: 117-123
- 7 Jarrell P.M., Fox C.E., Michael H., Webb S.L., *Practical Aspects of CO<sub>2</sub> Flooding*, 2002, *SPE Monogr. Ser. Vol. 22*.
- 8 La H., Guigard S.E., Extraction of hydrocarbons from Athabasca oil sand slurry using supercritical carbon dioxide, *J. Supercrit. Fluids*, 2015; 100: 146-154
- 9 Sagisaka M., Iwama S., Hasegawa S., Yoshizawa A., Mohamed A., Cummings S., Rogers S.E., Heenan R.K., Eastoe J., Super-Efficient Surfactant for Stabilizing Water-in-Carbon Dioxide Microemulsions, *Langmuir* 2011; 27: 5772-5780
- 10 Klostermann M., Strey R., Foster T., Sottmann T., Schweins R., Lindner P., Microstructure of supercritical CO<sub>2</sub>-in-water microemulsions: a systematic contrast variation study, *Phys. Chem. Chem. Phys.*, 2011; 13: 20289-20301
- 11 Heitz M.P., Carlier C., deGrazia J., Harrison K.L., Johnston K.P., Randolph T.W., Water Core within Perfluoropolyether-Based Microemulsions Formed in Supercritical Carbon Dioxide, *J. Phys. Chem. B*, 1997; 101: 6707-6714
- 12 Zielinski R.G., Kline S.R., Kaler E.W., Rosov N., A Small-Angle Neutron Scattering Study of Water in Carbon Dioxide Microemulsions, *Langmuir*, 1997; 13: 3934-3937
- 13 Dalvi V.H., Srinivasan V., Rossky P.J., Understanding the effectiveness of fluorocarbon ligands in dispersing nanoparticles in supercritical carbon dioxide, *J. Phys. Chem. C*, 2010; 114: 15553-15561
- 14 Dalvi V.H., Srinivasan V., Rossky P.J., Understanding the Relative Effectiveness of Alkanethiol Ligands in Dispersing Nanoparticles in Supercritical Carbon Dioxide and Ethane, *J. Phys. Chem. C*, 2010; 114: 15562-15573
- 15 Stone M.T., da Rocha S.R.P., Rossky P.J., Johnston K.P., Molecular Differences between Hydrocarbon and Fluorocarbon Surfactants at the CO<sub>2</sub>/Water Interface, *J. Phys. Chem. B* 2003 ;107: 10185-10192
- 16 Stone M.T., Smith P.G., da Rocha S.R.P., Rossky P.J., Johnston K.P., Low Interfacial Free Volume of Stubby Surfactants Stabilizes Water-in-Carbon Dioxide Microemulsions, *J. Phys. Chem. B*, 2004; 108: 1962-1966
- 17 Lau C., Butenhoff J.L., Rogers J.M., The developmental toxicity of perfluoroalkyl acids and their derivatives, *Toxicol. Appl. Pharmacol*, 2004; 198: 231-241
- 18 Butenhoff J., Costa G., Elcombe C., Farrar D., Hansen K., Iwai H., Toxicity of ammonium perfluorooctanoate in male cynomolgus monkeys after oral dosing for 6 months, *Toxicol. Sci.*, 2002; 69:

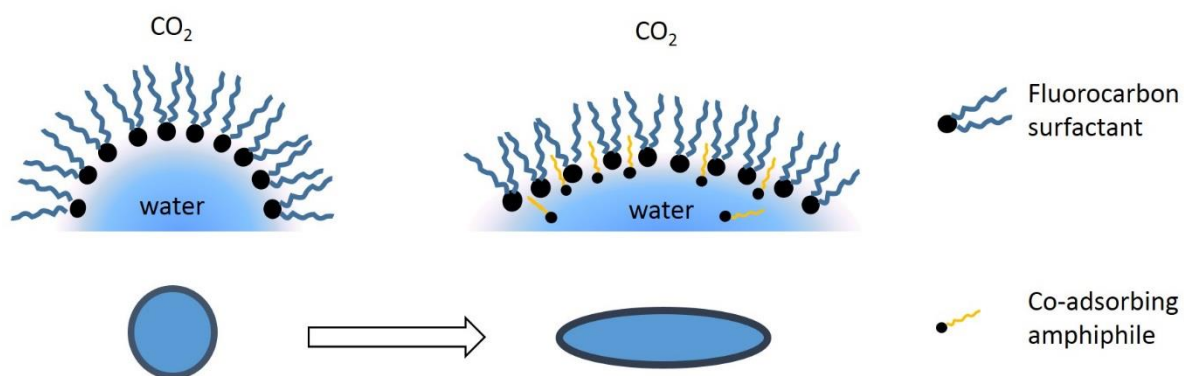


- 19 Houde M., Martin J.W., Letcher R.J., Solomon K.R., Muir D.C.G., Biological Monitoring of Polyfluoroalkyl Substances: A Review, *Environ. Sci. Technol.*, 2006; 40: 3463-3473
- 20 Hollamby M.J., Trickett K., Mohamed A., Cummings S., Tabor R.F., Myakonkaya O., Gold S., Roger S., Heenan R.K., Eastoe J., Tri-Chain Hydrocarbon Surfactants as Designed Micellar Modifiers for Supercritical CO<sub>2</sub>, *Angew. Chem. Int. Ed.*, 2009; 48: 4993-4995
- 21 Fan X., Ptluri V.K., McLeod M.C., Wang Y., Liu J., Enick R.M., Oxygenated Hydrocarbon Ionic Surfactants Exhibit CO<sub>2</sub> Solubility, *J. Am. Chem. Soc.*, 2005; 127: 11754-11762
- 22 Ma S.L., Wu Y.T., Enick R.M., Wallen S.L., Grant C.S., Sugar Acetates as CO<sub>2</sub>-philes: Molecular Interactions and Structure Aspects from Absorption Measurement Using Quartz Crystal Microbalance, *J. Phys. Chem. B*, 2010; 114: 3809-3817
- 23 Mohamed A., Ardyani T., Sagisaka M., Ono S., Narumi T., Kubota M., Brown P., James C., Eastoe J., Kamari A., Hashim N., Isa I.M., Baker S.A., Economical and Efficient Hybrid Surfactant with Low Fluorine Content for the Stabilisation of Water-in-CO<sub>2</sub> Microemulsions, *J. Supercrit. Fluids*, 2015; 101: 127-136
- 24 Cummings S., Enick R., Rogers S., Heenan R., Eastoe J., Amphiphiles for supercritical CO<sub>2</sub>, *Biochimie*, 2011; 94: 94-100
- 25 Mohamed A., Sagisaka M., Hollamby M., Rogers S.E., Heenan R.K., Dyer R., Eastoe J., Hybrid CO<sub>2</sub>-philic Surfactants with Low Fluorine Content, *Langmuir*, 2012; 28: 6299-6309
- 26 Sagisaka M., Ono S., James C., Yoshizawa A., Mohamed A., Guittard F., Rogers S.E., Heenan R.K., Yan C., Eastoe J., Effect of Fluorocarbon and Hydrocarbon Chain Lengths in Hybrid Surfactants for Supercritical CO<sub>2</sub>, *Langmuir*, 2015; 31: 7479-7487
- 27 Binks B.P., Fletcher P.D.I., Kotsev S.N., Thompson R.L., Adsorption and Aggregation of Semifluorinated Alkanes in Binary and Ternary Mixtures with Hydrocarbon and Fluorocarbon Solvents, *Langmuir*, 1997; 13: 6669-6682
- 28 Putz T., Grassberger L., Lindner P., Schweins R., Strey R., Sottmann T., Unexpected efficiency boosting in CO<sub>2</sub>-microemulsions: a cyclohexane depletion zone near the fluorinated surfactants evidenced by a systematic SANS contrast variation study, *Phys. Chem. Chem. Phys.*, 2015; 17: 6122-6134
- 29 Sagisaka M., Koike D., Mashimo Y., Yoda S., Takebayashi Y., Furuya T., Yoshizawa A., Sakai H., Abe M., Otake K., Water/Supercritical CO<sub>2</sub> Microemulsions with Mixed Surfactant Systems, *Langmuir*, 2008; 24: 10116-10122
- 30 Yan C., Sagisaka M., James C., Rogers S.E., Peach J., Hatzopoulos M.H., Eastoe J., Action of hydrotropes in water-in-CO<sub>2</sub> microemulsions, *Colloid & Surf. A*, 2015; 476: 76-82
- 31 Span R., Wagner W., A New Equation of State for Carbon Dioxide Covering the Fluid Region from the Triple-Point Temperature to 1100 K at Pressures up to 800 MPa, *J. Phys. Chem. Ref. Data*, 1996; 25: 1509-1596
- 32 Hollamby M.J., Practical applications of small-angle neutron scattering, *Phys. Chem. Chem. Phys.*, 2013; 15: 10566-19579
- 33 King S.M., Pethrick R.A. & Dawkins J.V. (editors), *Modern Techniques for Polymer Characterisation*, Wiley (1999)
- 34 Sears V.F., Neutron scattering lengths and cross section, *Neutron News*, 1992; 3: 26-37
- 35 Heenan R.K., Penfold J., King S.M., SANS at Pulsed Neutron Sources: Present and Future Prospects, *J. Appl. Crystallogr.*, 1997; 30: 1140-1147

- 
- 36 Heenan R.K., Rogers S.E., Turner D., Terry A E, Treadgold J K, Small Angle Neutron Scattering Using Sans2d, *Neutron News*, 2011; 22: 19-21
- 37 Wignall G.D., Bates F.S., Absolute calibration of small-angle neutron scattering data, *J. Appl. Crystallogr.* 1987; 20: 28-40
- 38 Guinier A., La diffraction des rayons X aux très petits angles: application a l'étude de phénomènes ultramicroscopiques, *Anales de Physique*, 1939; 12: 161-237
- 39 G. Porod, Die Röntgenkleinwinkelstreuung von dichtgepackten kolloiden Systemen, *Koll. Z.*, 1951; 124: 83-114
- 40 Hatzopoulos M.H., James C., Rogers S., Grillo I., Dowding P.J., Eastoe J., Effects of small ionic amphiphilic additives on reverse microemulsion morphology, *J. Colloid & Interface Sci.*, 2014; 421: 56-63
- 41 Hatzopoulos M.H., Eastoe J., Dowding P.J., Grillo I. Cylinder to sphere transition in reverse microemulsions: The effect of hydrotropes, *J. Colloid & Interface Sci.*, 2013; 392: 304-310
- 42 Yan C., Sagisaka M., James C., Rogers S.E., Alexander S., Eastoe J., Properties of surfactant films in water-in-CO<sub>2</sub> microemulsions obtained by small-angle neutron scattering, *J. Colloid & Interface. Sci.*, 2014; 435: 112-118
- 43 Kuttich B., Falus P., Grillo I., Stuhn B., Form fluctuations of polymer loaded spherical microemulsions studied by neutron scattering and dielectric spectroscopy, *J. Chem. Phys.*, 2014; 141: 084903
- 44 Schubel D., Ilgenfritz G., Influence of Polyethylene Glycols on the Percolation Behaviour of Anionic and Nonionic Water-in-Oil Microemulsions, *Langmuir*, 1997; 13: 4246-4250
- 45 Muller M., Stuhn B., Busse K., Kressler J., Modification of a reverse microemulsion with a fluorinated triblock copolymer, *J. Colloid & Interface. Sci.*, 2009; 335: 228-233

---

TOC Graphic



**For Graphical Abstract ONLY**